Chapter 8
Rapid Retrofitting of RC Columns Using Fe-SMA for Enhanced Seismic Performance

M. Sarmah, S. K. Deb, and A. Dutta

Abstract Collapse of many buildings and bridges in past earthquakes can be primarily attributed to damage in RC columns due to insufficient ductility. Studies have shown that addition of lateral confinement to concrete increases its strength and ductility significantly. Prestrained strips/wires (2–8%) made of shape memory alloy (SMA), a smart material, have recently gained popularity for their ability to provide in-situ active confinement of RC columns without the use of mechanical anchorages and in much lesser time. Prestrained SMAs can regain their original (undeformed) shape when heated above their transformation temperature. Thermal activation of prestrained SMA while restrained leads to the development of a large recovery stress, which is utilized to exert active confinement pressure externally on RC column. A low-cost iron-based SMA (Fe-SMA) is adopted for rapid retrofitting of RC column. A parametric study on behavior of Fe-SMA-confined concrete was carried out. It was found that the residual stress of Fe-SMA confined concrete is independent of concrete strength and only function of active confinement pressure on concrete. This material-level study was further expanded to the component-level for retrofitting of RC columns using Fe-SMA strips. Design of rapid retrofitting strategies of RC column using Fe-SMA strips in its plastic hinge region is discussed in this chapter.

Keywords Fe-SMA · Retrofitting · Shape memory effect · RC column

8.1 Introduction

There is a growing emphasis on the sustainability of existing structures. Due to this, a lot of research has been done on seismic repair and retrofitting of RC structures, which aims at improving their performance against seismic forces. Necessity for seismic retrofitting arises in non-ductile columns of RC structures, which were designed prior to the introduction of ductile detailing guidelines. These techniques may also be used

M. Sarmah · S. K. Deb (✉) · A. Dutta
Civil Engineering Department, IIT Guwahati, Assam 781039, India
e-mail: skdeb@iitg.ac.in

for upgradation of structures so as to fulfill the requirements of the latest reforms in codal practices and/or hazard levels. Other issues that may necessitate strengthening include aging of the structure, change in its usage and loading requirements, and deterioration of structural strength at local or global level due to poor maintenance or post-earthquake damage. Seismic retrofit strategies can broadly be divided into global and local retrofit strategies. Global retrofit strategies target the overall performance of the structure when subjected to lateral loads by addition of shear walls, infill walls, bracings, supplemental damping, and base isolation among others. Local retrofit strategies aim at enhancing the seismic resistance of a structural member without having a substantial impact on the overall resistance of the structure. These include jacketing of beams, columns, beam-column joints, strengthening of individual footings, etc. Retrofitting is a better alternative to replacement because it not only saves time and money but also helps in cutting CO_2 emissions in construction.

RC columns constructed prior to the introduction of ductile detailing code of practice are termed as substandard as they had insufficient ductility arising from inadequate transverse reinforcement and/or lap splice length at its plastic hinge region. Research studies have demonstrated that lack of flexural ductility and/or poor shear resistance are the key factors that cause the collapse of RC columns [1–4]. Over the last few decades, a significant number of studies have been carried out by researchers, which focused on the development of appropriate strengthening and repair techniques for RC columns. These techniques aim to fulfill the requirement of improved strength and ductility and lower the cost of implementation while ensuring minimum disruption to building occupants during retrofitting activities keeping the structure's aesthetics in mind. Another critical consideration is repair time, particularly for lifeline structures such as bridges and hospitals. Hence, there is a growing emphasis for the need of rapid strengthening and repair techniques.

The addition of lateral confinement to concrete has been proven to significantly increase the strength and ductility of the concrete. Richart et al. [5] first investigated the effect of lateral confinement on ductile failure of concrete. The findings of this study encouraged numerous other researchers to come up with alternative strategies to apply lateral confinement and access the behavior of concrete under these confinement methods. Concrete confinement methods can be divided into two types: passive and active. In case of passive confinement, the confining pressure develops gradually after dilation of the concrete during loading. Several researchers [6, 7] have studied the behavior of concrete confined by transverse reinforcement. For existing structures with poorly designed RC columns, additional (external) confinement for concrete is provided at the potential plastic hinge regions. This passive confinement is commonly applied using external reinforced concrete (RC) jackets [1, 8, 9], steel jackets [2, 10, 11], and fiber-reinforced polymer (FRP) [12–18].

In case of active confinement, the lateral confining pressure is applied to the concrete prior to its dilation. Although the methodology adopted by several researchers to apply active confinement on-site differed, majority of them sought to employ prestressed steel strands or FRP belts [19, 20]. The results demonstrated efficacy of retrofitting using active confinement strategies in enhancing shear capacity and ductility of the columns. This is because prior application of confinement pressure

causes a delay in the onset of damage in concrete. Even though active confinement is widely acknowledged to be superior to passive confinement, its implementation in the retrofitting strategies has been hindered. This is because such techniques result in many practical problems on-site related to use of specialized equipment and excessive amount of time and labor. As such, conventional passive confinement methods have become more viable in the construction industry. In light of the above, a smart material known as shape memory alloy (SMA) has lately gained popularity for use in active confinement of civil engineering structures.

By virtue of its unique thermo-mechanical property, shape memory effect (SME), prestrained SMAs can regain their original (undeformed) shape when heated above their transformation temperature. If the SMA is restrained while heating, large recovery stresses are developed in it, which in turn aids in prestressing the structural component against which it is restrained. Unlike conventional prestressing techniques, this method doesn't require heavy machinery on-site. Also, the time required for generation of recovery stress is much lesser.

The idea of employing SMA spirals for active confinement of concrete through thermal prestressing was initially presented by Andrawes and Shin [21]. Subsequently, several researchers [22–28] carried out experiments to study the behavior of concrete confined by NiTiNb SMA spirals. Results indicated an improvement in ultimate stress and strain of concrete. However, its widespread application was hindered owing to its high cost and complex production procedure. Hence, for prestressing structural elements at a low cost, a Fe-SMA with composition Fe–17Mn–5Si–10Cr–4Ni–1(V, C) (mass %) was developed in 2009 at the Swiss Federal Laboratories for Materials Science and Technology (Empa) [28].

Several studies have been carried out for characterization of this material [29–31]. In addition, several experimental investigations have shown that Fe-SMAs have a high potential for strengthening of structural components [32–34]. Recovery stresses of 300–350 MPa were developed after heating the Fe-SMA to 160 °C. Prestressing using Fe-SMA strips was found to be successful in improving the strength, ductility, and energy dissipation capacity of RC columns. In this chapter, design of rapid retrofitting strategies of RC column using Fe-SMA strips in its plastic hinge region will be discussed. Five SMA configurations, namely hoop, end-anchored (EA), near-surface mounted (NSM), combination of hoop and EA, and combination of hoop and NSM are highlighted.

8.2 Retrofitting Techniques Using Confinement Approach

Poor performance of structures during the past seismic events has drawn researchers in the field of structural retrofitting. One of the most common retrofitting techniques that are used to increase the strength and ductility of RC columns is provision of additional external confinement. These concrete confinement techniques can be categorized into two categories: (1) Passive confinement and (2) Active confinement. These are further elaborated in the following subsections.

8.2.1   Comparison of Stress–Strain Behavior of Passively and Actively Confined Concrete

The fundamental difference between passive and active confinement is the instant mobilization of lateral confining pressure. Figure 8.1a shows cross-sections of passively and actively confined concrete cylinders. As seen in the figure, lateral confining pressure is applied to the concrete section prior to axial loading in case of active confinement. However, in passive confinement technique, concrete has to dilate, i.e., deform laterally for mobilization of the confining pressure. Hence, early application of confinement pressure causes a delay in the onset of damage in actively confined concrete.
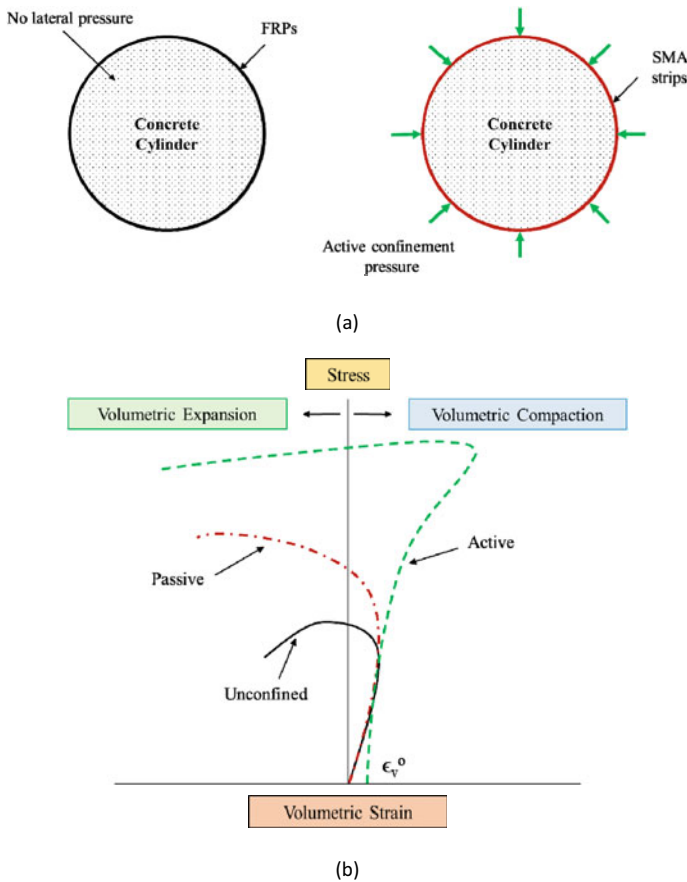

(a)

(b)

Fig. 8.1 Passive versus active confinement (**a**) cross-sections of passively and actively confined concrete before loading (**b**) stress versus volumetric strain curves of unconfined, passively, and actively confined concrete

Figure 8.1b illustrates the typical axial stress versus volumetric strain responses of unconfined, passively confined, and actively confined concrete. In the elastic region, the unconfined concrete undergoes volumetric compaction, following which there is rapid expansion leading to failure. Similarly, when passively confined concrete is subjected to axial stress, its volume decreases in the elastic region. As the axial stress increases, passive confining pressure aids in delaying the instant at which the concrete begins to expand volumetrically. However, in the active confinement case, the lateral confining pressure is mobilized on the concrete as a prestress before application of service loading. This leads to the development of an initial volumetric strain ε_v^o resulting from compaction. Additional axial stress is required in order to counteract the effect of this strain, thus delaying the failure of the concrete as compared to passively confined concrete.

8.2.1.1   RC Jacketing

RC jackets have been used to enhance the performance of vulnerable columns for several decades. In traditional RC jacketing, the original column cross-section is enlarged over a portion or its entire length using reinforced concrete. This new section is connected to the original section using dowel bars. Although this retrofitting technique improves the strength and ductility of the columns [1, 8, 9], it is labor intensive with a high operation cost owing to roughening, cleaning, and dowelling of the existing damaged concrete section so as to ensure composite deformation between the jacket and the column surface. It increases the size of the structural element, thereby changing its dynamic properties, which is likely to impose a higher seismic demand on the structure.

8.2.1.2   Steel Jacketing

Steel jacketing involves installation of a steel jacket by welding the components and using cement-based grout to fill the space between the jacket and the original or enlarged column. This technique was able to enhance the strength and ductility of the retrofitted columns resulting in considerably larger lateral loads and energy dissipation capacities as compared to the as-built columns [2, 9, 14]. Furthermore, similar to RC jacketing, this approach alters the stiffness of the structure by changing the cross-sectional dimension of the RC column section. This approach, however, has certain downsides, corrosion, and debonding being the common problems with the bonded sheets. There are also challenges involved in its transportation and installation in remote areas.

8.2.1.3 FRP Jacketing

In the recent decades, strengthening of RC columns by FRP composites has become increasingly popular. FRP comprises fibers (e.g., carbon, aramid, glass, etc.) connected effectively with the help of resins, which provide the mechanism for load transfer between the fibers and are responsible for composite strength. In FRP jackets, fibers are oriented in different directions to achieve different objectives. Fibers aligned along the longitudinal axis of the column increase its flexural strength, whereas those aligned in the transverse direction improve its shear capacity and ductility [12–17]. FRP composites have been more prevalent for retrofitting of RC columns as compared to RC and steel jackets. This is because of its high strength-to-weight ratio, which results in minimal modification of the geometry of RC columns while enhancing its capacity. Several disadvantages associated with the use of FRP confinement are its need for experienced workmanship, high cost, ineffective functioning in the compression part of cyclic loads and delamination.

8.2.2 Active Confinement Techniques

Active confinement, as compared to passive confinement, effectively slows down the lateral expansion of concrete under compression because the pressure is applied before the concrete dilates; hence increasing the ductility and strength of concrete. These attractive features encouraged many researchers to consider applying active confinement by the following techniques:

8.2.2.1 Triaxial Pressure Vessel/Triaxial Testing Machine

Most of the early studies on active confinement used triaxial testing devices to investigate the behavior of concrete. The study by Richart et al. [5] was one of the first studies on active confinement of concrete, which used fluids in a triaxial pressure vessel to exert a constant lateral confining pressure. The following equations were proposed to determine the peak strength f_{cc} and strain ϵ_{cc} of confined concrete under a lateral confining pressure f_l:

$$f_{cc} = f_{co} + k_1 f_l$$
$$\varepsilon_{cc} = \varepsilon_{co}\left(1 + k_2 \frac{f_l}{f_{co}}\right)$$

(8.1)

where f_{co} and ε_{co} are the peak strength and corresponding strain of the unconfined concrete and k_1 and k_2 are coefficient values that take into account the effect of active confining pressure. The suggested values for k_1 and k_2 are 4.1 and $5k_1$, respectively. Many analytical models have been built on the basis of these fundamental equations.

After the pioneering study by Richart et al. [5], several researchers conducted experiments on concrete blocks or cylinders under biaxial/triaxial stress using a triaxial testing machine. These studies demonstrated that the strength and the strain of concrete are dramatically improved by increasing the confining pressure.

8.2.2.2   Prestressing Steel Reinforcement/FRP Jackets

Active confinement was applied in the field by researchers using various methodologies. Some researchers adopted lateral prestressed steel strands and special anchorage devices for confinement of RC columns [19]. Others examined the feasibility of applying confining pressures with the help of prestressed FRP belts [20]. A key difference between using triaxial pressure vessel/triaxial testing machine and prestressed steel strands/FRP belts to apply active confining pressure is that the active confining pressures applied through the former remain constant throughout the test, whereas in the latter case, active confining pressure is exerted prior to loading and additional passive confining pressure keeps developing with concrete expansion during loading. Since it incorporates the advantages of both active and passive confinement techniques, it is found to effectively improve the axial and lateral capacity of RC columns. However, this technique requires complex maneuvering to apply the required external pressure. Hence, researchers began exploring for a simpler yet effective approach to apply active confinement on-site with minimal hardware and labor. This objective is fulfilled by the use of SMAs, details of which are elaborated in the next section.

8.2.2.3   SMA Confinement

The concept of employing SMAs to provide active confinement of concrete is based on utilizing the recovery stress generated upon thermal activation of SMAs. SMAs can regain their original shape even after undergoing excessive deformations up to 8% strain. By virtue of its unique thermo-mechanical property, shape memory effect (SME), prestrained SMAs can regain their original (undeformed) shape when heated above their transformation temperature. If the SMA is restrained while heating, large recovery stresses are developed in it, which in turn aids in prestressing the structural component against which it is restrained. The recovery stress is largely dependent on the SMA composition, manufacturing technique, and level of prestrain prior to shape recovery. The idea of employing SMA spirals for active confinement of concrete through thermal prestressing was initially presented by [21] Andrawes and Shin (2008). Prestrained SMA wires were wrapped around the plastic hinge region of the column and anchored at both ends. These were then heated using electric current or a fire torch. The induced shrinkage of the SMA wires causes a squeezing effect on the concrete column, which in turn provides active confinement to the column. Unlike

conventional prestressing techniques, this method doesn't require heavy machinery on-site. The effectiveness of this technique can be attributed to the thermo-mechanical properties of the SMAs, which will be discussed in the next section.

8.2.3   Shape Memory Alloys

Shape Memory Alloys (SMAs) are metallic alloys that deform significantly under external load at low temperatures and recover when heated over a particular temperature. This ability to remember its original undeformed shape lends this metallic alloy group its name, i.e., shape memory alloy and this phenomenon is referred to as shape memory effect (SME). Another thermo-mechanical phenomenon that is unique to these groups of alloys is known as superelasticity (SE). By virtue of SE, if this material undergoes substantial deformation by the action of external load, above a particular temperature, it is able to recover the same upon unloading. These distinctive properties of the SMAs, SME, and SE are related to the specific characteristics at the microstructural level that permits reversible solid–solid phase transformation among variants of its constituent phases, namely Martensite [M], and Austenite [A]. This was first discovered in 1951 in Au-Cd alloy, followed by the discovery of Ni–Ti alloy. These are divided into three major groups: NiTi-based, Cu-based, and Fe-based. SMAs are widely used in actuator applications, valves, pipe couplings, dampers, and medical applications. Majority of uses of SMAs are confined to military, aerospace, and medical applications. However, there has lately been a surge in demand for SMAs in civil engineering applications as well.
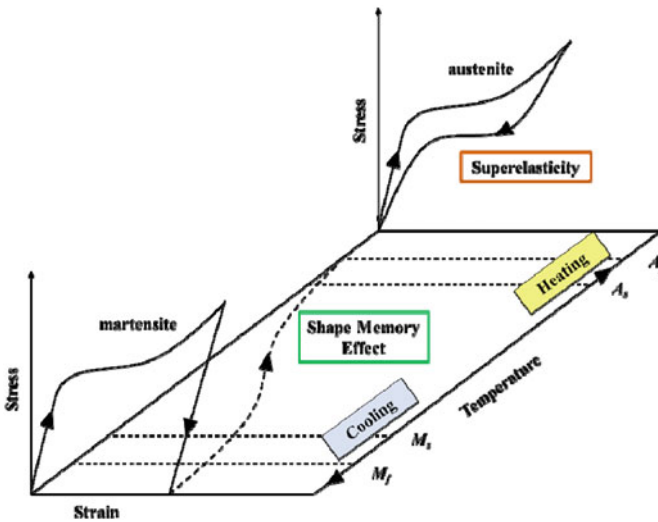
8.2.3.1   Thermo-Mechanical Properties of SMAs

SMAs have two main crystallographic phases, the low-temperature phase is called Martensite [M], and the high-temperature phase is called Austenite [A]. The regulations governing the transition from one phase to the next are highly dependent on the alloy's temperature in terms of four transformation temperatures, which are unique to each alloy as shown in Fig. 8.2(a). These transformation temperatures are (1) the martensite start temperature (M_s), where the martensitic transformation of austenite to martensite starts, (2) the martensite finish temperature (M_f), where the martensitic transformation of austenite to martensite finishes, and below Mf the SMAs are completely in martensite phase (3) the austenite start temperature (A_s), where the reverse transformation of martensite to austenite starts, (4) the austenite finish temperature (A_f), where the reverse transformation of martensite to austenite finishes, and beyond A_f, the SMAs are completely in austenite phase.

If an SMA is excessively deformed in the austenite phase, stress-induced martensite is formed. However, once the stress is removed, reverse transformation from martensite to austenite starts and the SMA returns back to its original shape. This phenomenon is known as superelasticity. A typical flag-shaped stress–strain behavior
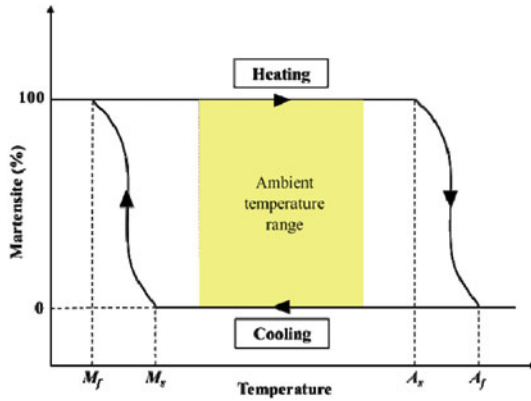
(a)

(b)

Fig. 8.2 Thermo-mechanical properties of SMA (**a**) phases (**b**) superelasticity and shape memory effect

of SMA loaded in the austenite phase is shown in Fig. 8.2b. As the loading and unloading paths are different, superelastic SMAs exhibit large hysteresis, which are utilized in civil structures as dampers and base isolation devices. When an SMA is deformed in its martensite phase, it is subjected to significant residual strains even after removal of loading. Upon heating up to above A_f, it recovers its original unde-formed shape as shown in Fig. 8.2b. This phenomenon is known as shape memory effect (SME). However, if the SMA is restrained, it will not be able to recover its

original shape and a recovery stress develops in the SMA. Researchers have made efforts to utilize this recovery stress of SMAs in the application of active confinement technique for concrete.

8.2.3.2 SMA Confinement Concept

The SMA confinement concept is illustrated in Fig. 8.3. Prestrained SMA wires/strips (2–8% prestrained by the manufacturer) are wrapped around concrete members, and heated to their activation temperature, while restrained, to activate SME. As the spiral is unable to restore its original length because of the restraining action of concrete, a large recovery stress is generated in it. This recovery stress squeezes the concrete member, exerting confining pressure on it.

Andrawes et al. [21] initially investigated the possibility of using SMA spirals for active confinement of concrete by thermal activation. Even at low confining pressures, uniaxial compression tests of concrete cylinders wrapped with NiTiNb SMA spirals revealed a considerable increase in concrete strength and ductility. Later, Shin and Andrawes [22–24] incorporated this study to experimentally investigate the retrofitting of RC columns using prestrained NiTiNb SMA spirals. The approach was found to be beneficial in improving the ductility and energy dissipation capacity of the RC columns. A retrofitting approach was proposed which employed SMA confinement to improve the ductility of concrete more efficiently as compared to conventional passive confinement techniques. Although the NiTi-based alloys are the most widely used SMAs, these are very expensive for large-scale applications. Hence, for prestressing structural elements at a low cost, an Fe-SMA with composition Fe–17Mn–5Si–10Cr–4Ni–1(V, C) (mass %) was developed in 2009 at the Swiss Federal Laboratories for Materials Science and Technology (Empa) [28]. For mobilization of active confinement pressure, this Fe-SMA strip is heated to 160 °C in less than 60 s. Because of the advantages offered by Fe-SMA for prestressing applications, a number of investigations have been conducted to further characterize this alloy [29–31]. Most of the experimental studies are conducted on strengthening and repair applications of RC beams [32–34]. To numerically analyze the performance of
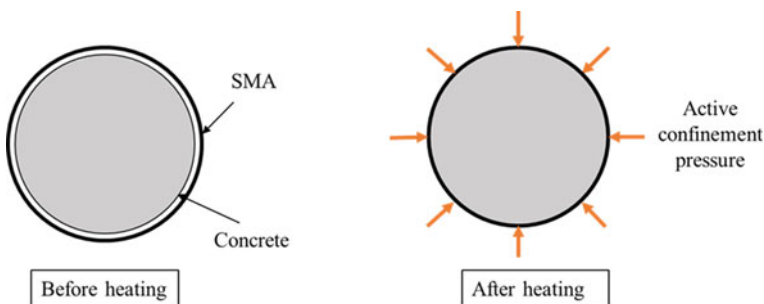

Fig. 8.3 Active confinement concept of SMA

RC beams with Fe-SMA as NSM reinforcement, Abouali et al. [35] developed a 3D nonlinear finite element model in ABAQUS. Results of these studies showed significant strengthening effect as compared to that of reference beam and that Fe-SMAs have a high potential for retrofit of structural components.

8.2.4   Fe-Based Shape Memory Alloys

The use of Fe-SMA strips for prestressing applications in RC members comprises three steps, which are shown in Fig. 8.4a:

1. Fe-SMA strips are initially prestrained to a specific strain level. After attainment of this strain level, it is fully released (Segment 1).
2. Fe-SMA strips are thermally activated by heating to their activation temperature while affixed on concrete surface or embedded in concrete (Segment 2).
3. When the RC member is loaded, the behavior of the Fe-SMA strips is as shown in Fig. 8.4a (Segment 3).

The recovery stress generation in the Fe-SMA strip during the above-mentioned steps is shown in Fig. 8.4b. At the beginning of the heating step, due to thermal expansion, the stresses in the Fe-SMA strip decrease. Upon attainment of the transition temperature, tensile stresses develop in the strips due to reverse transformation of the alloy from martensite state to austenite. Once the strip is cooled down to the room temperature, there is a further increase in its tensile stress due to thermal contraction. Since the Fe-SMA strips are restrained against concrete, compressive stresses develop in the concrete member. Phase change temperatures for the Fe-SMA
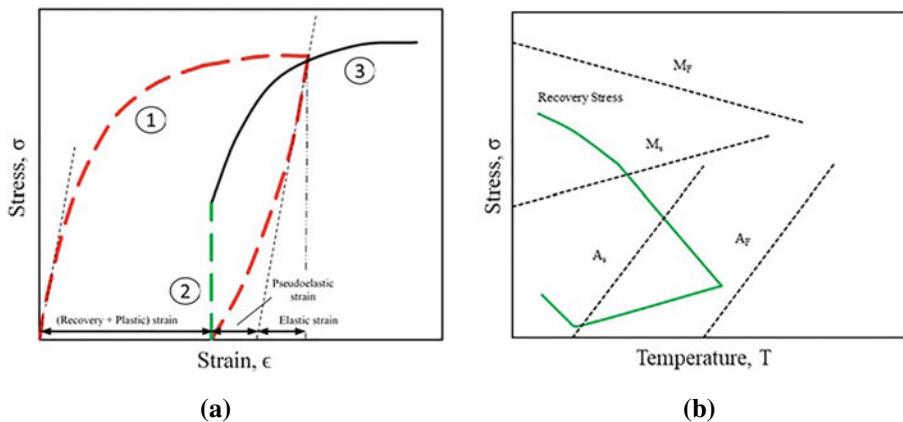

Fig. 8.4 Prestressing application of Fe-SMA (**a**) stress–strain behavior (**b**) recovery stress generation stress development

have been reported by Lee et al. [30] as follows: $M_f = -64\ °C$, $M_s = -60\ °C$, $A_s = 103\ °C$, and $A_f = 163\ °C$.

Shahverdi et al. [33] carried out material characterization of the Fe-SMA strips for the purpose of prestressing applications in civil engineering structures. The ultimate tensile strength and corresponding failure strain of the Fe-SMA strips was found to be 1000 MPa and 40%, respectively. This indicated that the strips have high strength as well as ductility. After heating the Fe-SMA strips to 160 °C, recovery stresses of 300–350 MPa were recorded. It was found that the recovery stresses generated after thermal activation depend on the prestrain level of the strips as well as the temperature of activation. A 2% prestrain level was found to be optimum for achieving maximum recovery stress at an activation temperature of 160 °C. These results are used for structural design purposes.

8.3 Parametric Study on Concrete Confined by Fe-SMA Strips

Abouali et al. [35] developed a 3D nonlinear finite element (FE) model in ABAQUS to numerically explore the strengthening of RC beams in flexure with NSM Fe-SMA strips. This modeling approach is used to numerically predict and analyze the behavior of concrete confined by Fe-SMA strips using FE method. Parametric studies are carried out to study the effect of two design variables: concrete strength and Fe-SMA strip spacing on the constitutive behavior of concrete. For this purpose, standard concrete cylinders of 150 mm diameter and 300 mm height were modeled for FE simulation. Three different concrete grades of characteristic strength 25, 30, and 40 MPa, which are designated as A, B, and C, respectively, are considered in this study.

To understand the effect of Fe-SMA strip spacing on the constitutive behavior of concrete, four different SMA strip spacing are adopted in the study. The dimensions of Fe-SMA strips used are 24 mm width and 1.5 mm thickness. Four different strip spacing of 92, 69, 55.2, and 46 mm, which are designated as S1, S2, S3, and S4, are considered in this parametric study. Hence specimen A-S1 implies M25 grade concrete cylinder with Fe-SMA spacing of 92 mm.

Previous studies on active confinement have shown that the axial stress–strain response of concrete under monotonic loading appears to be the envelope of axial stress–strain response of cyclically loaded concrete [36]. Hence in this study, the cylinders were subjected to monotonic loading only.

Active confining pressures corresponding to different strip spacing were calculated based on the effective confining pressure proposed by Mander et al. [7]. According to Mander et al. [7], for a circular section, the effective confining pressure $f_l{}'$ can be calculated as

$$f_l' = \frac{2k_e f_y A_{sp}}{sD} \tag{8.2}$$

where k_e is the confinement effectiveness ratio, f_h is the SMA recovery stress [36], A_{sp} and s are the cross-sectional area and center-to-center spacing of the Fe-SMA strip and D is the diameter of the specimen. Details of modeling in ABAQUS are discussed in the following sub-section.

8.3.1 Material Models

8.3.1.1 Concrete Constitutive Model

To model the behavior of concrete, the CDP model available in ABAQUS was used [35]. In this model, damage is incorporated both in tension as well as compression. Concrete having cylindrical compressive strength, $f_c{}'$ of 50 MPa and direct tensile strength, f_t of 2.4 MPa is used [16]. The stress–strain curve of concrete under uniaxial compression was defined using the Hognestad parabola [37], as described in Eq. (8.3):

$$\sigma_c^{(1)} = E_{c0}\varepsilon_c \text{ for } \sigma_c < 0.4 f_c'$$

$$\sigma_c^{(2)} = f_c'\left[2\left(\frac{\varepsilon_c}{\varepsilon_c'}\right) - \left(\frac{\varepsilon_c}{\varepsilon_c'}\right)^2\right] \text{ for } \frac{\varepsilon_c}{\varepsilon_c'} \le 1$$

$$\sigma_c^{(3)} = f_c' - \frac{f_c'\left(\varepsilon_c - \varepsilon_c'\right)^2}{\left(\varepsilon_{c,\max} - \varepsilon_c'\right)^2} \text{ for } \frac{\varepsilon_c}{\varepsilon_c'} > 1 \tag{8.3}$$

where σ_c and ε_c are the compressive stress and strain, respectively, $\varepsilon_{cm,ax}$ is the maximum strain, ε_c' is the strain corresponding to the peak stress, E_{co} is the modulus of elasticity of concrete. In tension, the stress-crack opening displacement curve postcracking of concrete was defined in the ABAQUS CDP model by an exponential function described by Eq. (8.4) [38]:

$$\frac{\sigma}{f_t} = f(\omega) - \frac{\omega}{\omega_c}f(\omega_c)$$

$$\text{where, } f(\omega) = \left[1 + \left(\frac{c_1\omega}{\omega_c}\right)^3\right]\exp\left(-\frac{c_2\omega}{\omega_c}\right) \text{ and } \omega_c = 5.14\frac{G_f}{f_t} \tag{8.4}$$

where ω is the crack opening displacement, ω_c is the crack opening displacement at which no stresses can't be transferred, $f(\omega)$ is a displacement function, G_f is the concrete fracture energy, and c_1 and c_2 are material constants.

The values of the plasticity parameters used in this study are summarized in Table 8.1. Compressive and tensile damage variables in the CDP model are defined as per Birtel et al. [39].

Table 8.1 Plasticity parameters for CDP model [39]

Dilation angle, Ψ (°)	50
Plastic potential eccentricity, ε	0.1
Stress ratio, σ_{b0}/σ_{c0}	1.16
Shape of the yielding surface, K_c	0.667
Viscosity parameter, μ	0.0001

8.3.1.2 Iron-Based Shape Memory Alloy (Fe-SMA) Strips

The Fe-SMA strips were modeled with the stress–strain curve obtained in the tension test [33], using isotropic hardening plasticity as shown in Fig. 8.5. For the concrete cylinders confined with activated Fe-SMAs, the loading to failure segment of the stress–strain diagram was implemented in the FE model.

8.3.2 Finite Element Model

Continuum eight-node linear brick elements with reduced integration and hourglass control (C3D8R) were used to model the concrete as it provides a solution of comparable accuracy as compared to second-order tetrahedral elements at less computational cost. Fe-SMA strips, as shown in Fig. 8.6, were modeled with two-node Timoshenko beam elements (B31) with linear interpolation as they can be subjected to large axial strains.

Assuming no slip between the SMA strips and concrete surface, a tie constraint was used to model the interaction between the two. A fixed boundary condition was applied to the bottom surface of the model during loading phase. Using the initial
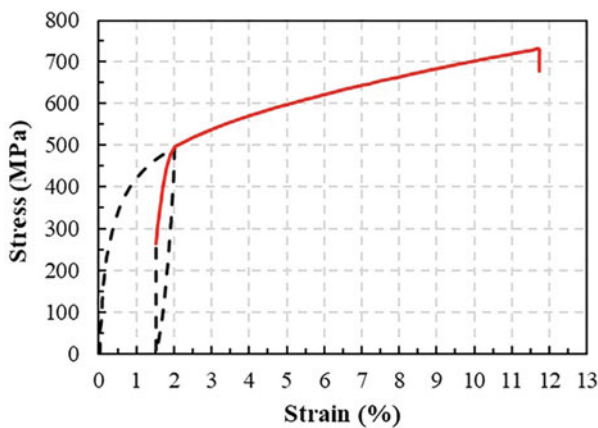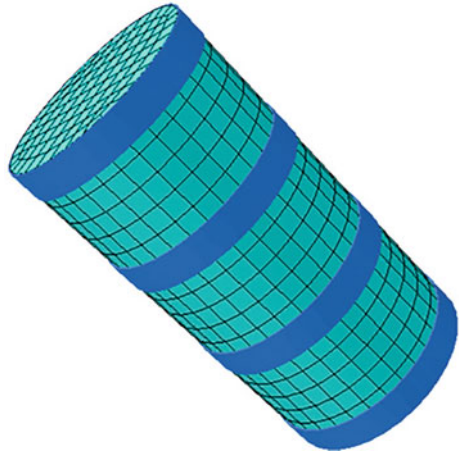

Fig. 8.5 Stress–strain curve of Fe-SMA

Fig. 8.6 FE model of concrete cylinder confined by Fe-SMA strips

stress feature in ABAQUS, the recovery stress was enforced as initial stress in the Fe-SMA strips in the axial direction. To allow establishment of self-equilibrium after assigning the initial stress, an idle step without any loading was defined.

Displacement-controlled loading was applied to the models by applying a monotonic vertical displacement with a loading strain rate of 0.5% per min until failure of the cylinder. The nonlinear solution was then obtained by configuring an implicit static general analysis method.

8.3.3 Results and Discussion

A parametric study is carried out to understand the effect of concrete strength and Fe-SMA strip spacing on the constitutive behavior of concrete. The results of all the specimens are summarized in Table 8.2.

8.3.3.1 Effect of Grade of Concrete

Four spacing values were considered in the study, namely, 92, 69, 55.2, and 46 mm. Figure 8.7 compares the axial stress–strain relationships of SMA confined concrete having same strip spacing with different concrete grades.

As the grade of concrete is increased from M25 to M40, it is observed that the peak stresses of A-S1, B-S1, and C-S1 increased by 51%, 45.3%, and 38.9%, respectively, as compared to that of their respective unconfined concrete specimens A, B, and C. However, residual stress of Fe-SMA confined concrete is found to be independent of concrete grade and is only a function of active confinement level for normal strength concrete. A similar trend is observed for specimens with SMA spacing of S2, S3, and S4. This observation is in agreement with the experimental results obtained by [27] for NiTiNb-SMA spirals confined concrete.

Table 8.2 Summary of results for all specimens

Specimen	Active confinement pressure (MPa)	f'_{cc} (MPa)	f_{res} (MPa)
A	0	19.6	–
A-S1	1.09	29.7	15.2
A-S2	1.76	33.9	21.9
A-S3	2.44	35.6	26.8
A-S4	3.14	45.2	32.7
B	0	23.5	–
B-S1	1.09	34.1	15.4
B-S2	1.76	38.3	22.1
B-S3	2.44	40.8	26.9
B-S4	3.14	49.5	32.8
C	0	30.9	–
C-S1	1.09	42.9	15.1
C-S2	1.76	47.1	22.1
C-S3	2.44	49.2	27.1
C-S4	3.14	58.1	32.9

8.3.3.2 Effect of Spacing of Fe-SMA Strips

As the spacing of Fe-SMA strips is decreased from S1 to S4, the effective confinement pressure exerted by the strips on concrete increases. With increasing value of confinement pressure, it is observed (Fig. 8.8) that the peak stresses of A-S1 to A-S4 increased by 51%, 72.9%, 81.6%, and 130%, respectively, as compared to that of the unconfined concrete specimen, A. From Fig. 8.8, it is evident that the ductility of the specimens also increases as compared to that of the unconfined specimen. Also, as established in the earlier section, residual stress is a function of confinement level of concrete. Thus, with increase in the confinement value of Fe-SMA strips the residual stress increases. A similar trend is observed for specimens of grade of concrete B, C when the spacing is varied from S2 to S4.

8.3.4 Observations Based on Parametric Study

This study focused on analyzing the behavior of SMA confined concrete using FEM within the framework of damaged plasticity model in ABAQUS. Active confinement of concrete is provided by prestrained Fe-SMA strips, which are restrained during heating. This is due to induction of large recovery stresses in the SMA, as it tries to recover its original undeformed configuration. This study is an initial step towards understanding the behavior of Fe-SMA confined concrete by numerically investigating the change in the constitutive behavior of concrete with changes in grade
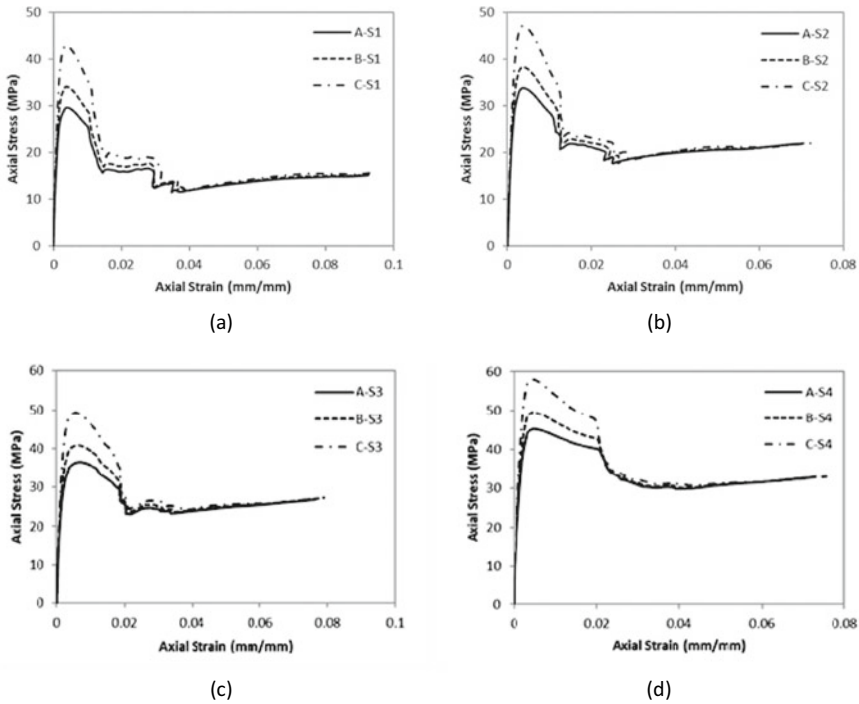
Fig. 8.7 Comparison of axial stress–strain relationships of Fe-SMA confined concrete of different grades (A = 25 MPa, B = 30 MPa and C = 40 MPa) for strip spacing (**a**) 92 mm (**b**) 69 mm (**c**) 55.2 mm (**d**) 46 mm

of concrete and SMA spacing. Concrete cylinders, 150 mm diameter and 300 mm height, having three different concrete grades of 25, 30, and 40 MPa and four different SMA strip-spacing of 92, 69, 55.2, and 46 mm were modeled and simulated under uniaxial compressive monotonic loading. The results show that there is an increase in the strength as well as ductility of the concrete specimens due to this active confinement.

The following conclusions could be drawn from the study:

1. The strength and ductility of Fe-SMA confined concrete increases as the active confinement pressure increases.
2. The residual stress of Fe-SMA confined concrete is independent of concrete strength and only function of active confinement pressure on concrete.
3. Therefore, it may be concluded that active confinement would provide enhanced seismic performance by increasing both strength and ductility of concrete.
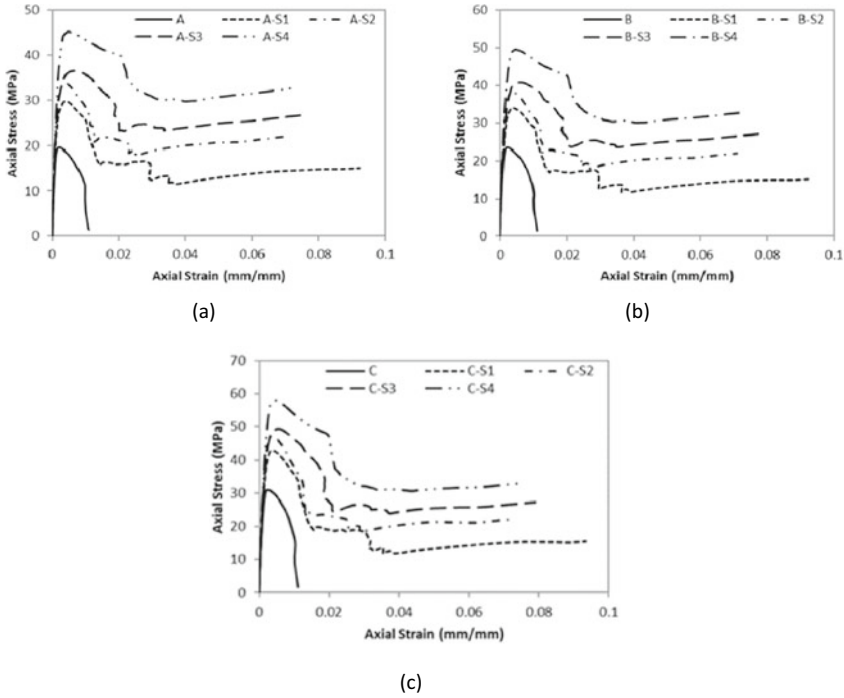
Fig. 8.8 Comparison of axial stress–strain relationships of Fe-SMA confined concrete having different strip spacing (S1 = 92 mm, S2 = 69 mm, S3 = 55.2 mm, and S4 = 46 mm) for concrete grades (**a**) 25 MPa (**b**) 30 MPa (**c**) 40 MPa

8.4 Design Methodology Adopted for Rapid Retrofitting Strategies of RC Columns Using Fe-SMA Strips

The parametric study presented in the previous section demonstrated the effectiveness of the active confinement technique using Fe-SMA strips in enhancing the strength and ultimate strain of concrete. This material-level study is further expanded to the component-level for retrofitting of RC columns using Fe-SMA strips.

Inelastic response of RC columns subjected to axial compression and bending is characterized by plastic deformations localized in small regions, namely the plastic hinge region. Under seismic events, the performance of plastic hinge regions of RC columns is extremely important as it governs its load-carrying and deformation capacities.

From a design perspective, additional confinement in RC columns should be provided along the length of its plastic hinge zones as shown in Fig. 8.9 so that the retrofitted RC columns can attain the desired ductility characteristics in order for them to survive severe seismic events. Hence, RC columns are retrofitted with thermally prestressed Fe-SMA spirals at the plastic hinge region as shown in Fig. 8.8.

Fig. 8.9 Retrofitting of RC
column using Fe-SMA strips
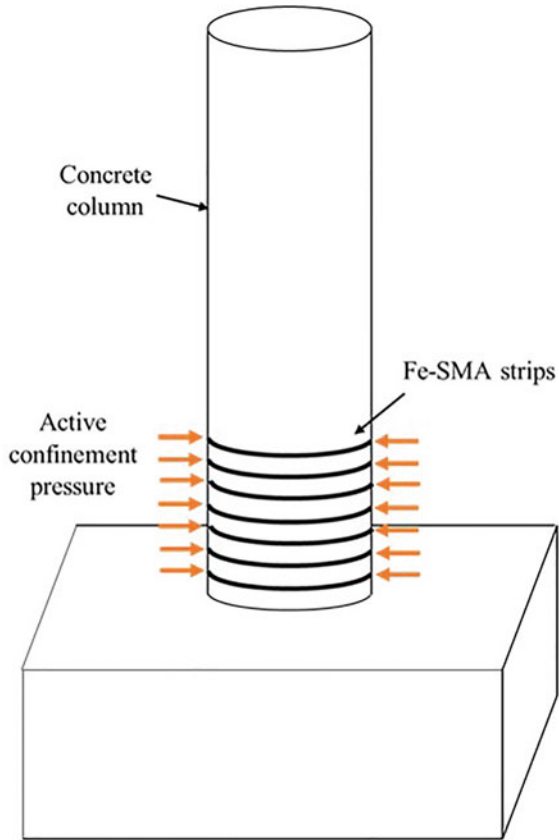
The length of the plastic hinge region where the SMA strips were applied is estimated
as (1) $l_p = 1.5$ times the column diameter [40] or (2) $l_p = 0.08L + 0.022d_b f_y$ [41]
where f_{sy} and $d_b =$ yield strength and bar diameter of the main column reinforcement,
respectively.

When SMA strips are used for confinement of RC columns, the total confining
pressure acting on it comprises two components: an active component and a passive
component. According to Mander et al. [7], for a circular section, the effective
confining pressure $f_l{}'$ can be calculated from Eq. (8.2). In this equation, f_h is the hoop
stress along the transverse reinforcement, which Mander et al. [7] assumed to be the
yield strength of transverse steel for internal transverse steel confined concrete.

The above-mentioned equation can be applied for SMA confinement to calculate
the effective active component of the total confining pressure from Fe-SMA strips by
using SMA recovery stress as the hoop stress. The passive component is calculated
using hoop stress that develops in the Fe-SMA strips during loading. Tensile test data
of Fe-SMA strips from Shahverdi et al. [33] can be utilized to calculate the hoop stress
along the strips when concrete dilates. When the level of active confinement decreases

to a certain level, it's efficiency in improving the strength and ductility of RC columns decreases. Chen et al. [36] recommended this limiting active confinement pressure to be 0.91 MPa.

The use of Fe-SMA strips for active confinement of RC columns facilitates rotation of the plastic hinge, thus preventing failure of the column-footing connection. Owing to early application of confinement pressure, prior to loading, Fe-SMA strips protect the concrete in the plastic hinge region of the RC column from early spalling hence delaying its damage. It also improves the energy dissipation of the RC column. However, this depends on the effective active confinement pressure, which in turn depends on the spacing of the Fe-SMA strips in the plastic hinge region. Specimens with higher confinement pressures perform better as compared to those with lower confinement pressures. The height of application of Fe-SMA strips is advised to be slightly higher than the height of the plastic hinge to minimize uncertainties for estimation of plastic hinge length.

8.5 Concluding Remarks

The present available retrofitting methods for RC columns (e.g., concrete or FRP jackets) cannot be implemented immediately after the occurrence of an earthquake. As a result, there is an urgent requirement for an efficient retrofitting method that can be executed in the field in less time. This can be fulfilled by the use of Fe-SMA strips for active confinement of RC columns. The time and labor required in this rapid retrofitting technique are minimal. Unlike using prestressed steel strands or FRP belts, installation of thermally prestressed Fe-SMA strips doesn't require heavy machinery. Thermal activation of prestrained SMA leads to the development of a large recovery stress, which is utilized to exert active confinement pressure externally on RC column on which it is fixed. A recovery stress of 350 MPa is generated in the Fe-SMA strips when it is heated to 160 °C. A parametric study was carried out to understand the behavior of Fe-SMA confined concrete by numerically investigating the change in the constitutive behavior of concrete with changes in grade of concrete and SMA spacing. It was found that the residual stress of Fe-SMA confined concrete is independent of concrete strength and only function of active confinement pressure on concrete. Active confinement using Fe-SMA strips would provide enhanced seismic performance by increasing both strength and ductility of concrete. From a design perspective, additional confinement in form of Fe-SMA strips provided along the plastic hinge length of RC columns can help in attainment of the desired ductility characteristics in order for it to survive severe earthquakes. The use of Fe-SMA strips for rapid repair takes only a few hours, which makes them very suitable for situations where performing emergency retrofit is required.

References

1. Bett B, Klingner R, Jirsa J (1988) Lateral load response of strengthened and repaired reinforced concrete columns. ACI Struct J 85:499–508
2. ChaiI YH, Priestley MN, Seible F (1991) Seismic retrofit of circular bridge columns for enhanced flexural performance. Struct J 88(5):572–584
3. Priestley MN, Seible F, Xiao Y, Verma R (1994) Steel jacket retrofitting of reinforced concrete bridge columns for enhanced shear strength-part 1: theoretical considerations and test design. Struct J 91(4):394–405
4. Priestley MN, Seible F, Xiao Y (1994) Steel jacket retrofitting of reinforced concrete bridge columns for enhanced shear strength–Part 2: test results and comparison with theory. Struct J 91(5):537–551
5. Richart FE, Brandtzæg A, Brown RL (1928) A study of the failure of concrete under combined compressive stresses. University of Illinois at Urbana Champaign, College of Engineering
6. Scott B, Park R, Priestley M (1982) Stress-strain behavior of concrete confined by overlapping hoops at low and high strain rates. J Proc 79(1):13–27
7. Mander JB, Priestley MJ, Park R (1988) Theoretical stress-strain model for confined concrete. J Struct Eng 114(8):1804–1826
8. Rodriguez M, Park R (1994) Seismic load tests on reinforced concrete columns strengthened by jacketing. Struct J 91(2):150–159
9. Fukuyama K, Higashibata Y, Miyauchi Y (2000) Studies on repair and strengthening methods of damaged reinforced concrete columns. Cement Concr Compos 22(1):81–88
10. Daudey X, Filiatrault A (2000) Seismic evaluation and retrofit with steel jackets of reinforced concrete bridge piers detailed with lap-splices. Can J Civ Eng 27(1):1–16
11. Saiidi MS, Wehbe NI, Sanders DH, Caywood CJ (2001) Shear retrofit of flared RC bridge columns subjected to earthquakes. J Bridg Eng 6(3):189–197
12. Saadatmanesh H, Ehsani MR, Li M-W (1994) Strength and ductility of concrete columns externally reinforced with fiber composite straps. Struct J 91(4):434–447
13. Sheikh SA, Yau G (2002) Seismic behavior of concrete columns confined with steel and fiber-reinforced polymers. Struct J 99(1):72–80
14. ElSouri AM, Harajli MH (2011) Seismic repair and strengthening of lap splices in RC columns: carbon fiber–reinforced polymer versus steel confinement. J Compos Constr 15(5):721–731
15. He R, Grelle S, Sneed LH, Belarbi A (2013) Rapid repair of a severely damaged RC column having fractured bars using externally bonded CFRP. Compos Struct 101:225–242
16. He R, Sneed LH, Belarbi A (2013) Rapid repair of severely damaged RC columns with different damage conditions: an experimental study. Int J Concr Struct Mater 7(1):35–50
17. He R, Sneed LH, Belarbi A (2014) Torsional repair of severely damaged column using carbon fiber-reinforced polymer. ACI Struct J 111(3)
18. Rutledge ST, Kowalsky MJ, Seracino R, Nau JM (2014) Repair of reinforced concrete bridge columns containing buckled and fractured reinforcement by plastic hinge relocation. J Bridg Eng 19(8):A4013001
19. Saatcioglu M, Yalcin C (2003) External prestressing concrete columns for improved seismic shear resistance. J Struct Eng 129(8):1057–1070
20. Nesheli KN, Meguro K (2006) Seismic retrofitting of earthquake-damaged concrete columns by lateral pre-tensioning of FRP belts. In: Proceedings of the eighth US national conference on earthquake engineering
21. Andrawes B, Shin M (2008) Seismic retrofitting of bridge columns using shape memory alloys. In: Active and passive smart structures and integrated systems 2008, vol 6928. International Society for Optics and Photonics, p 69281K
22. Shin M, Andrawes B (2010) Experimental investigation of actively confined concrete using shape memory alloys. Eng Struct 32(3):656–664
23. Shin M, Andrawes B (2011) Lateral cyclic behavior of reinforced concrete columns retrofitted with shape memory spirals and FRP wraps. J Struct Eng 137(11):1282–1290

24. Shin M, Andrawes B (2011) Emergency repair of severely damaged reinforced concrete columns using active confinement with shape memory alloys. Smart Mater Struct 20(6):065018
25. Choi E, Chung Y-S, Choi J-H, Kim H-T, Lee H (2010) The confining effectiveness of NiTiNb and NiTi SMA wire jackets for concrete. Smart Mater Struct 19(3):035024
26. Dommer K, Andrawes B (2012) Thermomechanical characterization of NiTiNb shape memory alloy for concrete active confinement applications. J Mater Civ Eng 24(10):1274–1282
27. Chen Q, Andrawes B (2017) Cyclic stress–strain behavior of concrete confined with NiTiNb-shape memory alloy spirals. J Struct Eng 143(5):04017008
28. Dong Z, Klotz UE, Leinenbach C, Bergamini A, Czaderski C, Motavalli M (2009) A novel Fe–Mn–Si shape memory alloy with improved shape recovery properties by VC precipitation. Adv Eng Mater 11(1–2):40–44
29. Leinenbach C, Kramer H, Bernhard C, Eifler D (2012) Thermo-mechanical properties of an Fe–Mn–Si–Cr–Ni–VC shape memory alloy with low transformation temperature. Adv Eng Mater 14(1–2):62–67
30. Lee W, Weber B, Feltrin G, Czaderski C, Motavalli M, Leinenbach C (2013) Stress recovery behaviour of an Fe–Mn–Si–Cr–Ni–VC shape memory alloy used for prestressing. Smart Mater Struct 22(12):125037
31. Ghafoori E, Hosseini E, Leinenbach C, Michels J, Motavalli M (2017) Fatigue behavior of a Fe–Mn–Si shape memory alloy used for prestressed strengthening. Mater Des 133:349–362
32. Soroushian P, Ostowari K, Nossoni A, Chowdhury H (2001) Repair and strengthening of concrete structures through application of corrective posttensioning forces with shape memory alloys. Transp Res Rec 1770(1):20–26
33. Shahverdi M, Czaderski C, Motavalli M (2016) Iron-based shape memory alloys for prestressed near-surface mounted strengthening of reinforced concrete beams. Constr Build Mater 112:28–38
34. Michels J, Shahverdi M, Czaderski C, Schranz B, Motavalli M (2017) Iron based shape memory alloy strips, part 2: flexural strengthening of RC beams. Proc SMAR
35. Abouali S, Shahverdi M, Ghassemieh M, Motavalli M (2019) Nonlinear simulation of reinforced concrete beams retrofitted by near-surface mounted iron-based shape memory alloys. Eng Struct 187:133–148
36. Chen Q, Andrawes B (2017) Plasticity modeling of concrete confined with NiTiNb shape memory alloy spirals. In: Structures, vol 11. Elsevier, pp 1–10
37. Hognestad E (1951) Study of combined bending and axial load in reinforced concrete members. University of Illinois at Urbana Champaign, College of Engineering
38. Cornelissen H, Hordijk D, Reinhardt H (1986) Experimental determination of crack softening characteristics of normalweight and lightweight. Heron 31(2):45–46
39. Birtel V, Mark P (2006) Parameterised finite element modelling of RC beam shear failure. In: ABAQUS users' conference, vol 14
40. Caltrans C (2013) Seismic design criteria (SDC), v 1.7. California Department of Transportation, Sacramento, CA
41. Priestley MN, Seible F, Calvi GM (1996) Seismic design and retrofit of bridges. Wiley